

Article

Design and Test of Sensor for Monitoring Corn Cleaning Loss

Dexin Wei ¹, Chongyou Wu ^{1,*}, Lan Jiang ¹, Gang Wang ¹ and Hui Chen ²

¹ Nanjing Institute of Agricultural Mechanization, Ministry of Agriculture and Rural Affairs, Nanjing 210014, China

² Yancheng Dafeng Huiyang Agricultural Machinery Manufacturing Co., Ltd., Yancheng 224100, China

* Correspondence: wuchongyou@caas.cn

Abstract: At present, Chinese corn grain harvesters lack cleaning loss monitoring. Cleaning parameters cannot be automatically adjusted, and the loss rate is high. In view of the above problems, a cleaning loss monitoring sensor is designed, composed of a metal impact plate, piezoelectric ceramic and signal processing circuit. The factors affecting the characteristics of vibration signals are analyzed from the material, size and other aspects. The sensitive plate is composed of a 304 stainless steel impact plate and piezoelectric ceramic. The sensitive plate can convert the vibration signal of the impact plate into a voltage signal, and the output voltage range can reach ± 3 V or more. The signal generated by the collision of corn kernel and damaged corn cob with the sensitive plate was analyzed. It was found that the frequency domain range of corn grains was wider, with signals above 6 kHz, but broken corncobs did not have such signals. Based on the frequency distribution, a signal processing circuit is designed, which consists of high-pass filter circuit, an envelope detection circuit, and a voltage comparison circuit. The circuit can convert analog signals into pulse signals, which facilitates the counting process by the microprocessor. In order to obtain the monitoring accuracy and installation parameters of the integrated corn cleaning loss monitoring sensor, a Central Composite Design was carried out with the installation height and angle of the sensitive plate as the test factors and monitoring accuracy as the test index. Based on the test results and field test conditions, a regression model was established to determine the optimal installation parameters: the installation angle of the sensitive plate is 30° , and the installation height is 30 cm. At this stage, the accuracy of the sensor monitoring corn grains was 92.82%, and the accuracy of monitoring the mixture of corn grains and broken corncobs was 90.07%. The verification test shows that the monitoring accuracy can reach more than 94% after the sensor is debugged. This research can provide a reference for the design of corn cleaning loss monitoring devices.

Keywords: corn grains; loss monitoring sensors; signal processing; sensitive plate



Citation: Wei, D.; Wu, C.; Jiang, L.; Wang, G.; Chen, H. Design and Test of Sensor for Monitoring Corn Cleaning Loss. *Agriculture* **2023**, *13*, 663. <https://doi.org/10.3390/agriculture13030663>

Academic Editor: Filipe Neves Dos Santos

Received: 10 January 2023

Revised: 3 March 2023

Accepted: 9 March 2023

Published: 13 March 2023



Copyright: © 2023 by the authors. Licensee MDPI, Basel, Switzerland. This article is an open access article distributed under the terms and conditions of the Creative Commons Attribution (CC BY) license (<https://creativecommons.org/licenses/by/4.0/>).

1. Introduction

Harvesting is an important part of the corn production process. Corn grain harvesters can complete multiple processes such as ear picking, peeling, threshing, cleaning, and straw crushing in one operation. In recent years, due to its simplicity, convenience and high efficiency, it has rapidly developed in China. However, at present, the loss rate and crushing rate of most corn grain harvesters cannot meet the requirements of the new national standard [1,2]. Moreover, the loss rate of harvester cannot be monitored during the working process. The corn cleaning loss monitoring sensor can obtain the cleaning loss during the harvest operation in real time [3]. Therefore, the design of loss monitoring sensors is of great significance in realizing the precise control of cleaning parameters and intelligent operation.

As early as the 1970s and 1980s, the United States, Canada and other developed countries began to study crop cleaning loss monitoring sensors. The main focus of the study was on the sensor installation location [4,5] and signal processing [6,7]. With the development of computer miniaturization and high efficiency, Sharanakumar and Gilbert [8,9] used a

microcomputer to build a prediction model for the cleaning loss of a rice combine harvester. After years of research, the cleaning loss monitoring sensor has been installed on some harvesters according to customer needs. However, it is mainly applicable to monitoring the cleaning loss of single-cropped corn with low moisture content. Single-cropped maize has a long growth period, and the grain moisture content is relatively low at harvest. However, in Huang-Huai-Hai and other regions of China, maize is grown according to the double-cropping system, and the grain moisture content is about 30% at harvest. The density of corn kernels and corn cob with a moisture content below 24% is lower compared to those with a moisture content above 30%. In terms of the obtained signals, the main difference is shown in the similarity of signals generated by the collision between high-moisture corn kernels and broken cobs on the sensitive plate, making it more difficult to distinguish. Therefore, the loss monitoring sensor suitable for single-cropped maize cannot be directly introduced.

At the end of the last century, scholars in China studied the cleaning loss monitoring sensor. Wang Xinzong et al. [10] analyzed and studied the dynamic characteristics of the grain impact sensitive plate, calculated the vibration frequency generated by the grain impact sensitive plate, and concluded that the vibration frequency generated by the grain impact sensitive plate was different from the machine vibration frequency. The team of Mao Hanping [11,12] carried out a modal analysis on the sensitive plate, determined the sensor array arrangement, and obtained the cleaning loss monitoring sensor of rice combine harvester with good monitoring effect. Zhou Xianlong [13] designed a multi-point triggered grain cleaning loss monitoring sensor, which can effectively reduce the influence of machine vibration and noise, obtain a higher signal quality and improve the accuracy of monitoring. Wei Chuncai [14] designed an integrated multi-block rapeseed cleaning loss monitoring sensor. The contact force and contact time generated by rapeseed collision are higher than those of impurities, and the sensor also has a greater response to grain collision. However, most of the domestic research is for wheat, rice and other crop cleaning loss monitoring sensors [15,16], and the research on cleaning loss monitoring sensors for corn is insufficient [17].

In this paper, aiming at the lack of a loss monitoring device for corn grain harvester, the signal difference caused by the material composition of the corn grain harvester and the collision-sensitive plate between heavy impurities and grains is analyzed. A loss monitoring sensor composed of a piezoelectric ceramic, metal impact plate and signal processing circuit is designed. Finally, the monitoring accuracy and optimal working parameters of the sensor are verified by experiments.

2. Materials and Methods

2.1. Cleaning Discharge Composition Analysis

In order to fully understand the actual situation of the cleaning loss of corn grain harvester, and to collect indoor test materials, corn mechanical harvesting site sampling was carried out at a corn harvesting site in a farm in Yancheng City, Jiangsu Province, in September 2021. The operating machine was Lovol GE40. During the sampling process, it was found that the heavy impurities such as corn grains and broken corncobs screened out by the cleaning sieve were shaken out by the cleaning sieve, and the light impurities such as weeds and bracts were blown out by the fan inside the cleaning chamber. The light impurities were blown far away and almost never fell on the sensitive plate. Even if they fell on the sensitive plate, the signal generated was very weak. Therefore, only the corn grains and broken corncobs in the discharge were collected for signal acquisition and indoor test.

The collected materials are the effluents from the operation of the corn grain harvester. The length, width and thickness of 50 corn grains were measured, and the mean values were calculated. The results were 11.91 mm in length, 8.54 mm in width and 4.71 mm in thickness. The maximum size of the corn grains was length, and the maximum value was 14.41 mm. However, the physical properties such as volume and shape of broken corncobs

are very different. In the case of the same density, the broken corncobs with large size will affect the monitoring effect. Therefore, the broken corncobs are divided into three categories: large, medium and small. The large-sized broken corncobs are defined as two sizes greater than 20 mm in three sizes; the small-sized broken corncobs are defined as three sizes less than 15 mm; and the rest are medium-sized broken corncobs. The collected materials were mixed for statistics, and the results are shown in Table 1.

Table 1. Composition of effluent.

Component	Weight/(g)	Weight Percentage/(%)	Quantity	Quantity Percentage/(%)
Light impurity	286.52	5.41	—	—
Large-sized broken corncobs	2149.16	40.56	1446	32.33
Medium-sized broken corncobs	1465.42	27.66	1077	24.08
Small-sized broken corncobs	1283.07	24.22	1604	35.86
Corn grains	113.93	2.15	346	7.73

From Table 1, it can be seen that most of the materials in the discharge are broken corncobs, while the proportion of corn grains in weight and quantity is small. In order to reduce the impact of broken corncobs on monitoring accuracy, a screening device can be installed between the cleaning outlet and the monitoring sensor. Only the corn grains and small-sized broken corncobs pass through, while the large-sized broken corncobs and medium-sized broken corncobs are screened and directly fall to the ground. Figure 1a shows large-sized broken corncobs, and Figure 1b shows small-sized broken corncobs.



Figure 1. Broken corncobs: (a) Large-sized broken corncobs; (b) Small-sized broken corncobs.

2.2. Design and Development of Monitoring Sensor

2.2.1. Sensitive Plate Design

The loss monitoring sensor is composed of a sensitive plate and a signal processing circuit. The sensitive plate is composed of an impact plate and a piezoelectric ceramic. The impact plate is used to undertake the impact of corn grains and broken corncobs to form vibration signals. The piezoelectric ceramic is pasted on the back of the impact plate to convert the vibration signal into an electrical signal.

The design of the sensitive plate includes the material, size, structure, method of fixing of the impact plate and the installation position of the piezoelectric ceramic. Because the attenuation speed, vibration frequency and strain of the vibration of the impact plate are the main factors affecting the quality of the signal, the designed impact plate should have the characteristics of fast attenuation speed, high vibration frequency and large strain. The faster the attenuation, the lower the probability of interference by other signals in its signal cycle, so the higher the attenuation rate can effectively reduce the impact between signals. The larger the strain, the greater the peak voltage of the output electrical signal of the conversion element, and the easier it is to distinguish the vibration signal generated by the impact plate of different substances. The higher the signal frequency generated by the corn grains collision impact plate, the more effective it can distinguish the vibration noise frequency of the harvester and reduce the signal interference [18].

The literature review [19] found that 304 stainless steel as the impact plate material produces a better signal quality; impact plate design parameters are as follows (Table 2):

Table 2. Important parameters of impact plate.

Items	Parameter	Items	Parameter
Length	200 mm	Material	304 stainless steel
Width	200 mm	Fixing method	Bolting
Thickness	1 mm	Other processing	Four-sided bending

Piezoelectric ceramic is a commonly used conversion element in grain loss monitoring devices, such as piezoelectric ceramic buzzer due to its characteristics of fast response, fast signal attenuation, and large piezoelectric coefficient. The most important advantage of piezoelectric ceramic is its ability to adapt to the poor working environment in the field. It is a typical active element that converts mechanical energy into electrical energy through the piezoelectric effect. The main parameters of the selected piezoelectric ceramic sheet are shown in Table 3, and the structure is depicted in Figure 2. The piezoelectric ceramic serves as the positive electrode, and the negative output voltage signal is generated by the copper sheet.

Table 3. Main parameters of piezoelectric ceramics.

Parameters	Symbol	Numerical Values
Coupling coefficient	kp	0.68
Relative permittivity (F/m)	ϵ	1700
Piezoelectric constant (C/N)	d ₃₁	195
Elastic flexibility coefficient(m ² /N)	S ₃₃	19.2
Quality factor	Q _m	50
Dielectric loss	tg	0.02
Thickness (mm)	d	0.2
Radius (mm)	r	9

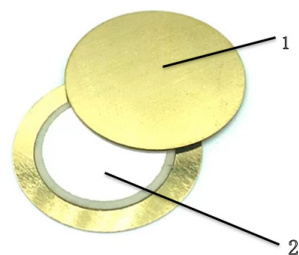


Figure 2. Piezoelectric ceramic sheet: 1—Copper sheet; 2—Piezoelectric ceramics.

When the piezoelectric ceramic is subjected to external force F , a charge q with opposite polarity and equal charge will appear on its two polar surfaces, so it can be regarded as a charge generator in parallel with a capacitor C_a . The definitions of terms used in Formulas (1)–(3) are shown in Table 3.

$$q = d_{31} \times F, \quad (1)$$

$$C_a = (\epsilon \times S)/d, \quad (2)$$

The output voltage of the piezoelectric ceramic as the voltage source is U :

$$U = (d_{31} \times F \times d)/(\epsilon \times S), \quad (3)$$

2.2.2. Signal Acquisition and Analysis

In order to design an accurate and efficient signal processing circuit, it is necessary to understand the characteristics of the signal generated by the core and grain collision-sensitive plate.

In this experiment, the signals generated by the collision-sensitive plate of broken corncobs and corn grains were collected 30 times, respectively, and there was no other vibration or noise interference in the collection process. The instruments and equipment used in the test include the sensitive plate, TBS1104 oscilloscope and tape. When the signal is collected, the sensitive plate is installed on the frame at a 45° tilt from the horizontal plane, and a single corn grain and the broken corncob fall freely from the top 40 cm to the sensitive plate. During the test, the time base of the oscilloscope is set to 10.0 ms, the total sampling time is 100ms, and the voltage range is set to -3 to 3 V. The sampling frequency of the oscilloscope under these settings is calculated to be $f_s = 2500/100 \text{ ms} = 25,000 \text{ Hz}$, where 2500 is the storage depth of the oscilloscope.

The collected vibration signal is a time domain signal, which describes the relationship between the output voltage of piezoelectric ceramic and time. The time domain waveform is the curve of the output voltage changing with time. In order to further understand and observe the signal characteristics through the measured signal, it is necessary to obtain the frequency domain signal. The Fourier Transform is used to transform the time domain signal into the frequency domain signal, and the frequency, amplitude and phase of the signal are obtained [20,21]. According to Nyquist's law, the spectrum in the range of $f = f_s/2 = 12,500 \text{ Hz}$ can be analyzed within the sampling range. The time domain and frequency domain signals of corn grains and broken corncobs after transformation are shown in Figure 3.

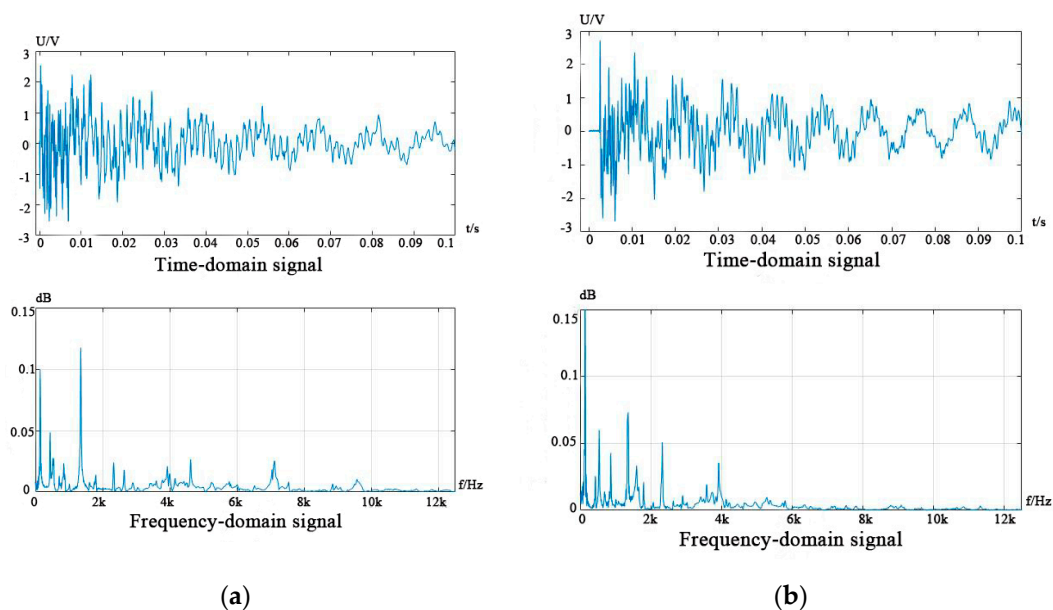


Figure 3. Time domain diagram and frequency domain diagram: (a) Time domain diagram and frequency domain diagram of signal generated by grains collision; (b) Time domain diagram and frequency domain diagram of signal generated by corncobs collision.

By observing and analyzing the collected 60 sets of signals, the amplitude intensity and frequency domain distribution of the signals generated by the corn grains collision and the signals generated by the broken corncobs collision are compared. It is found that there is no significant difference in the peak voltage of the two signals, but there is a certain difference in the frequency domain distribution. The main frequencies of the corn grains signal and broken corncobs signal are concentrated below 2 kHz or less, but the corn grain signal has a frequency of more than 6 kHz, while the broken corncob signal does not.

2.2.3. Signal Processing Circuit Design

The microprocessor cannot count the vibration signal directly output by the sensitive plate, and the signal processing circuit is needed to convert the vibration signal into a digital signal that the microprocessor can recognize. First, the function of signal processing circuit is to identify the corn grains signal, that is, filtering vibration, broken corncobs and other low-frequency interference signals, retain the high-frequency signal of the corn grains. The second is to convert the identified corn grains signal processing into a digital signal, so that the microprocessor can count the lost corn grains.

The signal processing circuit [22,23] is usually composed of charge amplification circuit, filter circuit, pulse shaping circuit and so on. Based on the design of the sensitive plate and the work of other researchers, this paper optimizes and improves the accuracy and efficiency of the loss monitoring sensor. Since the output voltage of the selected piezoelectric ceramic is relatively large, no charge amplification is required. The high-pass filter circuit can be used to filter out the low-frequency signal of the broken corncobs, and only the high-frequency signal of the corn grains is retained. The envelope detection circuit and voltage comparison circuit convert the filtered signal into a digital signal.

(1) High-pass filter circuit design

The high-pass filter circuit is used to retain the high-frequency signal of the corn grains and remove the broken corncobs signal. The cutoff frequency f_0 of the filter is set to be greater than the signal frequency generated by the broken corncobs, while the normal corn grains signal frequency is greater than f_0 . According to the analysis results of Section 2.2.2, the cutoff frequency f_0 is set to 8 kHz as the reference value of the high-pass filter circuit. The order of the filter will affect the bandwidth of the transition band. The rising rate of the first-order high-pass filter is 20 dB per ten-fold octave, and the rising rate increases by 20 dB for each additional order. Therefore, increasing the filter order can effectively reduce the bandwidth of the transition band. The introduction of positive feedback filter can increase the magnification, so that the cutoff frequency f_0 close to the characteristic frequency f_p . In summary, this study uses the voltage-controlled voltage source second-order active high-pass filter circuit shown in Figure 4, also known as VCVS high-pass filter circuit. The transfer function of the filter circuit is:

$$A_u = \frac{u_0}{u_i} = \frac{A_{up} [-(2\pi)^2 R_1 C_1 R_2 C_2 f^2]}{1 + j2\pi [R_1(C_1 + C_2) + (1 - A_{up})R_2 C_2] f - (2\pi)^2 R_1 C_1 R_2 C_2 f^2} \quad (4)$$

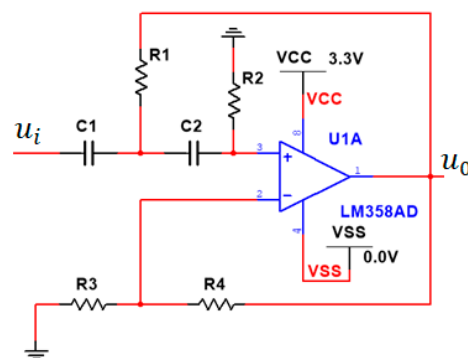


Figure 4. Second order active high-pass filter circuit of voltage controlled voltage source.

The characteristic frequency is:

$$f_p = \frac{1}{2\pi\sqrt{R_1 C_1 R_2 C_2}} \quad (5)$$

According to the original signal voltage range, microprocessor security voltage requirements, the amplifier supply voltage of 3.3 V. According to the design manual of the filter [24–26], when the order $K = 2$, the normalized coefficient of the VCVS high-pass filter is $B = 1.414$, $C = 1.00$, and the value of C_1 is close to $10/f_0 \mu\text{F}$. The resistance calculation formula is as follows (6)–(9).

$$R_2 = \frac{4C}{\left[B \div \sqrt{B^2 \div 8C(K-1)} \right] \omega_C C_1} \quad (6)$$

$$R_1 = \frac{C}{\omega_C^2 C_1^2 R_2} \quad (7)$$

$$R_3 = \frac{KR_2}{K-1} \quad (8)$$

$$R_4 = K \times R_2 \quad (9)$$

(2) Envelope detection circuit design

The envelope detection circuit is shown in Figure 5, which mainly utilizes the unidirectional conductive characteristics of the diode and the charging and discharging process of the detection load to complete the extraction of the modulation signal. The product of capacitance C_3 and resistance R_5 is the time constant. When the time constant has a suitable value, the output voltage corresponding to the envelope of the input voltage signal can be obtained. Therefore, the capacitance and resistance of the envelope detection circuit have a crucial impact on the performance of the circuit. According to the design experience, the time constant RC should satisfy $1/\omega \ll RC$, where ω refers to the frequency of the signal, and the resistance is generally above $50\text{K}\Omega$, and the capacitance is at the nF level or above.

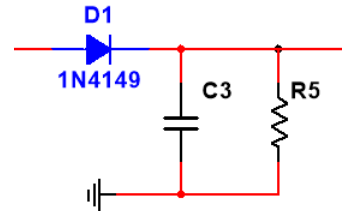


Figure 5. Envelope detection circuit.

(3) Voltage comparison circuit design

The voltage comparison circuit is shown in Figure 6, which is a circuit for identifying and comparing input signals. Its output has only low-level and high-level two states, so the analog signal can be converted into a digital signal [27]. When the forward input voltage of the operational amplifier is higher than the reverse input voltage, the voltage comparator output is high. Conversely, the output is low-level 0V. The operational amplifier used in this study is LM358. By adjusting the resistance of R_6 and R_7 , the trigger level of the voltage comparator can be adjusted, which means the width (duty cycle) of the collected vibration signal can be adjusted to adjust the detection time of each corn grains. In order to facilitate the adjustment, R_6 is selected as a sliding rheostat.

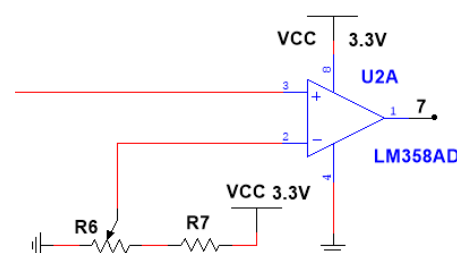


Figure 6. Voltage comparison circuit.

(4) Simulation and test

The NI Multisim14.0 software was used for simulation optimization analysis. After the signal processing circuit was completed in the software, a voltage source named ‘Piecewise Linear Voltage Source’ was added to import the collected time-domain signal values using this type of voltage source. Three dual-channel oscilloscopes were placed in the circuit. One channel of each oscilloscope was connected to the voltage source, and the other channel was connected to the output end of each part of the circuit. The simulation was carried out. Figure 7 shows the change process of the signal generated by the corn grains collision-sensitive plate. Additionally, Figure 8 shows the change process of the signal generated by the broken corncobs collision-sensitive plate. From left to right, the figures show the change in the signal through the high-pass filter circuit, the envelope detection circuit, and the voltage comparison circuit. Based on the simulation results, it was found that the filter circuit can effectively filter out the low-frequency signal of the broken corncobs and retain the high-frequency signal of the corn grains. The filtered signal can output the pulse signal through the envelope detection circuit and the voltage comparison circuit, and by adjusting the sliding variable resistor, the high- and low-level signal ratio of the output pulse signal is almost the same, which is convenient for the microprocessor to count.

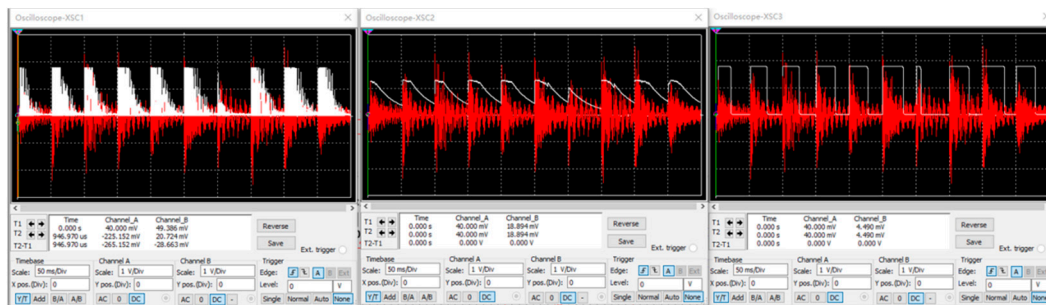


Figure 7. Change process of grain signal.

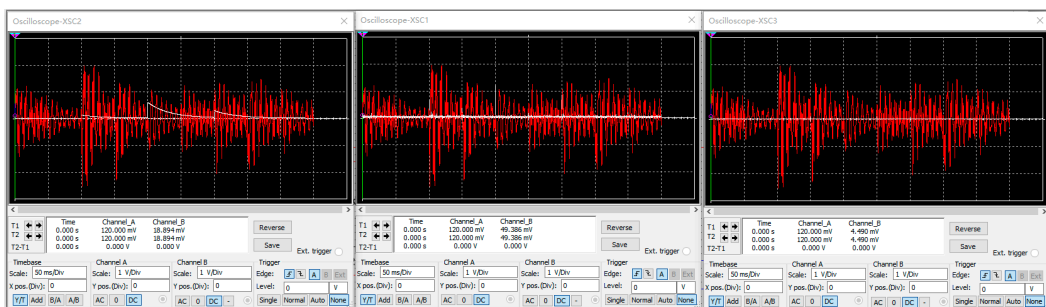


Figure 8. Change process of corncobs signal.

According to the designed signal processing circuit, the PCB board is made. Each circuit board has five signal processing circuits and one power input. The output end of the sensitive board signal is connected to the input end of the signal processing circuit to form a loss monitoring sensor, as shown in Figure 9.

The oscilloscope was used to observe the changes in signals generated by corn grains and broken corncobs collision-sensitive plate through various parts of the circuit. It was found that the signal change process was similar to the simulation results. Using the microprocessor to receive the signal output, when the small-sized broken corncobs collided with the sensitive plate, the microprocessor did not produce a count. However, when large-sized broken corncobs collided with the sensitive plate, there was a certain probability that the microprocessor would produce a count, so it was necessary to install a screening device above the sensitive plate. However, when corn grains collided with the sensitive plate, there was a certain probability that the microprocessor would not produce a count, resulting

in missed detection. Therefore, during the test, certain measures need to be taken to correct the relationship between the number of monitoring and the number of actual losses.

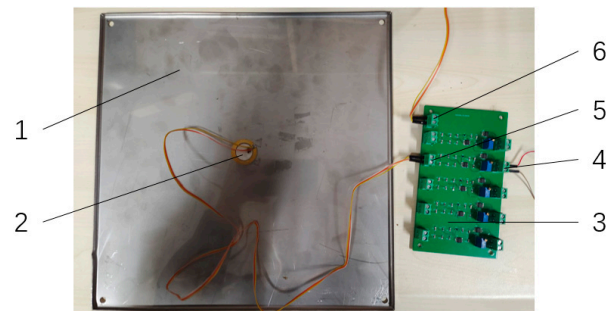


Figure 9. Structure of loss monitoring sensor: 1—Metal impact plate; 2—piezoelectric ceramics; 3—signal processing circuit PCB; 4—signal output terminal; 5—signal input terminal; 6—power input terminal.

2.3. Sensor Test

2.3.1. Test Conditions

In order to verify the working performance and design reliability of the designed sensor, and to determine the optimal installation position and angle of the loss monitoring sensor, a bench test was carried out in the laboratory. The test device and instrument mainly include conveyor belt, microcontroller, loss monitoring sensor, DC power supply etc., as shown in Figure 10. The conveyor belt device has two parts: one is the feeding device, which is used to send the material to the conveyor belt; the other is a conveying device, which collides the material with a certain horizontal speed to the sensitive plate.

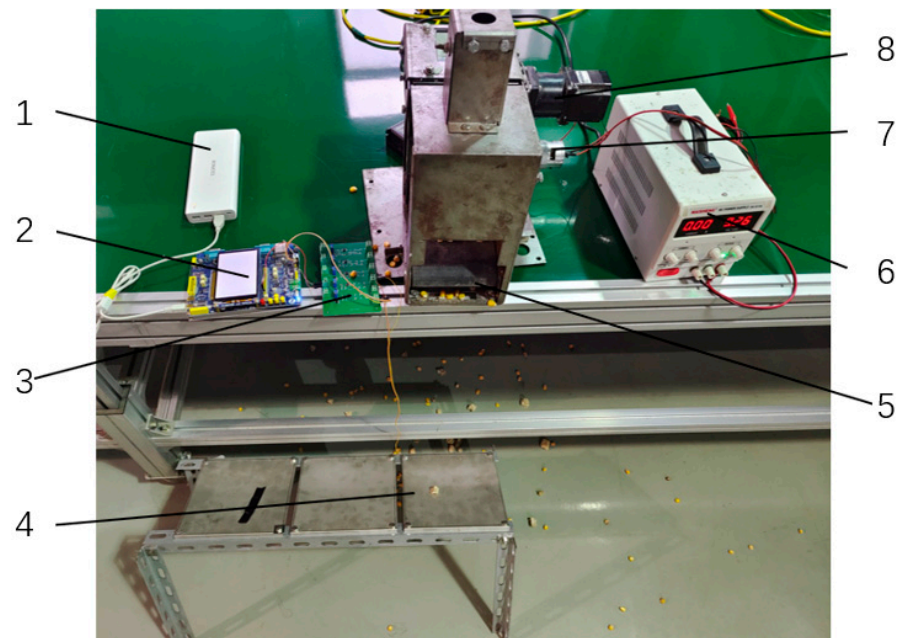


Figure 10. Test device: 1—5V DC power supply; 2—microprocessor; 3—signal processing circuit; 4—sensitive plate; 5—conveyor belt; 6—adjustable DC power supply; 7—DC motor1; 8—DC motor2.

The material used in the test has two parts: one part is all corn grains, and the other part is 10% corn grains mixed in with 30% medium-sized broken corncobs and 60% small-sized broken corncobs, where the proportion is the quantity proportion. The moisture content of maize grain was 31.11%. Both parts of the material were prepared using 200~300 grains, and the test process conveyor will produce a certain noise, without vibration interference.

2.3.2. Test Method

The installation height and angle of the sensitive plate can affect the monitoring accuracy of the sensor. Harvester outlet from the ground has a height of about 1 m, the sensitive plate should not be too close to the ground and the outlet, and the distance from sensitive plate to the outlet is 0.3~0.5 m; the installation angle of the sensitive plate is the angle between the sensitive plate and the horizontal plane. The larger the installation angle, the smaller the horizontal projection area of the sensitive plate, and the smaller the probability of corn grains collision. The smaller the installation angle β , the easier it is for the corn grains or broken corncobs to accumulate on the sensitive plate after collision, so the installation angle is 30~60°.

Taking the installation height and installation angle of the sensitive plate as the test factors, and the monitoring accuracy of the sensor as the test index, a Central Composite Design is carried out. The test factor coding is shown in Table 4.

Table 4. Test factor code.

Levels	Installation Angle A/(°)	Installation Height B/(cm)
−1.414	24	26
−1	30	30
0	45	40
1	60	50
1.414	66	54

3. Results and Analysis

This study designed a two-factor five-level Central Composite Design; the test plan uses 11 test points, including 4 spindle points, 4 orthogonal points, and 3 center points. Each group of tests is repeated three times to take the average value. This was performed in order to study the interaction between various factors to find the best installation position of the sensor. The test response value is shown in Table 5. Among them, the monitoring accuracy Y_1 indicates the monitoring accuracy of the sensor when the material is all corn grains, and the monitoring accuracy Y_2 indicates the monitoring accuracy of the sensor when the material is a mixture of corn grains and broken corncobs.

Table 5. Design of experiment and test results.

No.	Installation Angle A/(°)	Installation Height B/(cm)	Monitoring Accuracy Y_1 /%	Monitoring Accuracy Y_2 /%
1	30	50	87.04	84.86
2	30	30	92.82	90.07
3	60	50	83.17	78.33
4	60	30	86.17	82.50
5	66	40	84.02	79.35
6	24	40	92.56	88.05
7	45	26	89.30	87.32
8	45	54	84.35	79.75
9	45	40	86.80	82.47
10	45	40	87.09	82.94
11	45	40	86.63	83.03

We used Design-Expert13 software to statistically analyze both factors and establish the regression model, and we obtained the quadratic polynomial regression model of the monitoring accuracy Y_1 and the monitoring accuracy Y_2 for the installation angle A and the installation height B of the sensitive plate, as shown in Equations (10) and (11).

$$Y_1 = 86.78 - 2.84A - 1.98B + 0.70AB + 0.70A^2 - 0.05B^2, \quad (10)$$

$$Y_2 = 82.57 - 3.32A - 2.52B + 0.26AB + 0.66A^2 - 0.57B^2, \tag{11}$$

The variance analysis table of monitoring accuracy Y_1 and monitoring accuracy Y_2 is established, as shown in Table 6. The P-value of the regression model of monitoring accuracy Y_1 and monitoring accuracy Y_2 is less than 0.01, which proves that the regression model has a significant functional relationship with the independent variable. The lack of fit p -value > 0.1 proves that the regression model has a high degree of fitting. Factors A, B, $A \times B$ and $A \times A$ had a significant effect on monitoring accuracy Y_1 , while $B \times B$ had no significant effect on monitoring accuracy Y_1 . Factors A, B, $A \times A$ and $B \times B$ had a significant effect on monitoring accuracy Y_2 , while $A \times B$ had no significant effect on monitoring accuracy Y_2 . The mismatched terms of the regression model are not significant, indicating that the model is consistent with the test data.

Table 6. Variance analysis of regression equation.

Source of Variance	Monitoring Accuracy Y_1 /%					Monitoring Accuracy Y_2 /%				
	Sum of Squares	Degree of Freedom	Mean Square	F Value	p Value	Sum of Squares	Degree of Freedom	Mean Square	F Value	p Value
Model	100.31	5	20.06	86.72	<0.0001	142.43	5	28.49	139.03	<0.0001
A	63.78	1	63.78	275.74	<0.0001	87.20	1	87.20	425.58	<0.0001
B	31.16	1	31.16	134.71	<0.0001	50.39	1	50.39	245.94	<0.0001
$A \times B$	1.93	1	1.93	8.35	0.0233	0.27	1	0.27	1.32	0.2884
$A \times A$	3.31	1	3.31	14.30	0.0069	2.90	1	2.90	14.18	0.0070
$B \times B$	0.02	1	0.02	0.07	0.8033	2.21	1	2.21	10.77	0.0135
Residual	1.62	7	0.23			1.43	7	0.20		
Lack of fit	0.86	3	0.29	1.50	0.3432	0.78	3	0.26	1.58	0.3265
Pure error	0.76	4	0.19			0.66	4	0.16		
Correct total	101.93	12				143.87	12			

Figure 11a shows the response surface of the sensor’s monitoring accuracy Y_1 when the installation angle and installation height of the sensitive plate are both corn grains. When the installation angle is fixed at a certain level, the monitoring accuracy Y_1 decreases with the increase in installation height, and the decrease rate increases with the increase in installation angle. When the installation height is fixed at a certain level, the monitoring accuracy Y_1 decreases with the increase in installation angle, and the decreasing rate increases with the increase in installation height angle. Figure 11b is the response surface of the installation angle and installation height of the sensitive plate to the monitoring accuracy Y_2 of the sensor when the material is a mixture of corn grains and broken corncobs. The influence of various factors on the monitoring accuracy Y_2 is similar to Y_1 .

In order to determine the optimal location parameters of the sensor installation, the optimization module of Design-Expert13 software is used to optimize the regression model above with constrained objectives, with the objective function of $F(x)$ and the constraint function of $G(x)$.

$$F(x) = \begin{cases} \max Y_1(A, B) \\ \max Y_2(A, B) \end{cases} \tag{12}$$

$$G(x) = \begin{cases} 30 < A < 60 \\ 30 < B < 50 \end{cases} \tag{13}$$

The installation parameters when the monitoring accuracy of the sensor reaches the highest are as follows: the installation height is 30 cm away from the miscellaneous port, and the installation angle is 30° . At this stage, the monitoring accuracy Y_1 is 92.82%, and the monitoring accuracy Y_2 is 90.07%.

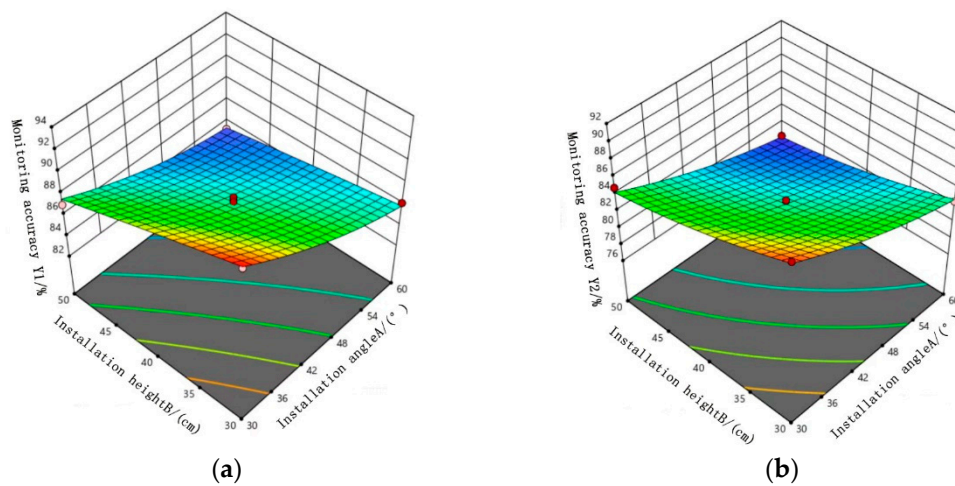


Figure 11. Response surface: (a) Response surface of various factors to monitoring accuracy Y_1 ; (b) Response surface of various factors to monitoring accuracy Y_2 .

On 12 October 2022, a field verification test was carried out in Dafeng District, Yancheng City, Jiangsu Province when the sensor was in the best installation parameters. As shown in Figure 12, the test machine was a LEVO GE40. During the experiment, the harvester was artificially fed, and the total weight of corn ears fed each time was about 10 kg. The number of grains lost by cleaning and the number of grains monitored were counted. After many experiments, the relationship between the number of cleaning lost grains and the number of grains monitored was continuously corrected, and the monitoring accuracy of the sensor could reach more than 94%.



Figure 12. Field test: 1—LEVO GE40 harvester; 2—Cleaning miscellaneous mouth; 3—Loss monitoring sensor.

4. Conclusions

By analyzing the proportion of cleaning discharge components in corn grain harvesters, the loss monitoring sensor composed of a sensitive board and signal processing circuit is determined. The signal generated by the collision of corn grains and broken corncobs was analyzed to select a square sensitive plate made of 304 stainless steel, with a thickness of 1mm and a side length of 200 mm. The signals generated by the collision of corn kernel and broken corn cob with the sensitive plate were collected. It was found that compared with the broken corn cob signal, the corn kernel had a signal greater than 6 kHz.

According to the signal difference between corn grains and broken corncobs, a signal processing circuit composed of a high-pass filter circuit, an envelope detection circuit and

a voltage comparison circuit is designed. Through simulation, it is found that the signal generated by the broken corncobs collision-sensitive plate cannot pass the filter circuit, while the signal of most corn grains can pass and finally generate pulse signals. After making the circuit board, it is verified that the actual results are the same as the simulation results.

Through theoretical analysis, the main factors affecting monitoring accuracy were determined, and test indicators for monitoring accuracy were established. Test factors for the sensitive plate installation angle and installation height were designed using a center combination test with two factors and three levels. A mathematical regression model was established using two factors and test indicators. Considering the test results and the actual operational situation, the optimal installation parameters of the sensor were determined to be an installation angle of 30° and an installation height of 30 cm, resulting in a monitoring accuracy of 90.07%. The verification test shows that the monitoring accuracy of the sensor can reach more than 94% after debugging, which can basically meet the application requirements.

Author Contributions: Conceptualization, C.W. and G.W.; methodology, C.W.; software, L.J.; validation, H.C. and C.W.; formal analysis, D.W.; investigation, D.W.; resources, H.C. and C.W.; data curation, C.W.; writing—original draft preparation, D.W.; writing—review and editing, D.W.; visualization, D.W.; supervision, C.W.; project administration, C.W.; funding acquisition, H.C. All authors have read and agreed to the published version of the manuscript.

Funding: This research was funded by Jiangsu Provincial Agricultural Science and Technology Independent Innovation Fund SCX (22) 2010, Institute-level basic scientific research business expenses project of Chinese Academy of Agricultural Sciences (S202204) and Subei Science and Technology Special Project of Jiangsu Province (SZ-YC202010).

Institutional Review Board Statement: Not applicable.

Informed Consent Statement: Informed consent was obtained from all subjects involved in the study.

Data Availability Statement: The data presented in this study are available on request from the authors.

Acknowledgments: The authors thank the editor and anonymous reviewers for providing helpful suggestions for improving the quality of this manuscript.

Conflicts of Interest: The authors declare no conflict of interest.

References

1. Wang, Z. *Design of Threshing and Separating Device about Corn Grain Harvester and Automatic Control System of Entrainment Loss*; Jiangsu University: Zhenjiang, China, 2021.
2. Guo, Y.; Zhan, P.; Li, X.; Zhu, J. Study on yield loss of maize during harvesting in China—Based on the surveys in 5 counties of 5 provinces. *J. Maize Sci.* **2018**, *26*, 130–136.
3. Zhang, M.; Jiang, L.; Wu, C.; Wang, G. Design and test of cleaning loss kernel recognition system for corn combine harvester. *Agronomy* **2022**, *12*, 1145. [[CrossRef](#)]
4. Edwin, M.N.; David, L.M.; Lyle, S.J. Grain Loss Monitor. U. S. Patent 3935866, 3 February 1976.
5. Osselaere Guy, H.J. Offset Grain Loss Sensor for Combine Harvesters. U.S. Patent 4540003, 10 September 1985.
6. Diekhans, N.; Willi, B. Lost-Grain Detector for Harvesting Machine. U.S. Patent 4902264, 20 February 1990.
7. Thomas, G.K. Acoustic Grain Flow Rate Monitor. U. S. Patent 4004289, 18 January 1977.
8. Hiregoudar, S.; Udhaykumar, R.; Ramappa, K.T.; Shreshta, B.; Meda, V.; Anantachar, M. *Artificial Neural Network for Assessment of Grain Losses for Paddy Combine Harvester a Novel Approach*; Springer: Berlin/Heidelberg, Germany, 2011; pp. 221–231.
9. Gilbert, J.; Strubbe, I. Grain Loss Monitors for Harvesting Machines. U. S. Patent 5046362, 10 September 1991.
10. Wang, X.; Zhang, S. Grain impact dynamics analysis of combine harvester grain loss sensor. *J. Agric. Mech. Res.* **1997**, *2*, 57–60.
11. Ni, J.; Mao, H.; Li, P. Design of Intelligent grain cleaning losses monitor based on array piezocrystals. *Trans. Chin. Soc. Agric. Mach.* **2010**, *41*, 175–177.
12. Mao, H.; Ni, J. Finite element analysis and measurement for array piezocrystals grain losses sensor. *Trans. Chin. Soc. Agric. Mach.* **2008**, *39*, 123–126.
13. Zhou, X. *Study on the Monitoring System for Cleaning Loss of the Grain Combine Harvester*; Northwest A&F University: Yangling, China, 2010.
14. Wei, C. *Study on the Monitoring Method and Device for Cleaning Loss of the Rapeseed Combine Harvester*; Jiangsu University: Zhenjiang, China, 2018.

15. Chun, W.; Ming, L.; Liangjun, Y.; Zhu, L. Research on loss monitoring of grain cleaning in combine harvester based on kalman filter. *J. Agric. Mech. Res.* **2016**, *38*, 23–27.
16. Zhang, G.; Jin, C.; Yang, T.; Liu, Z.; Chen, M.; Zhou, D. Design and implementation of cleaning loss rate monitoring system for combine harvester. *J. Chin. Agric. Mech.* **2019**, *40*, 146–150.
17. Yanhan, W.; Xiaoyu, L.; Enrong, M.; Du, Y.; Yang, F. Design and development of monitoring device for corn grain cleaning loss based on piezoelectric effect. *Comput. Electron. Agric.* **2020**, *179*, 105793.
18. Wei, C.; Li, Y.; Xu, L.; Liang, Z.; Wang, J. Design and experimental study of large feed quantity crawler full feeding rice combine harvester. *J. Agric. Mech. Res.* **2018**, *8*, 70–74.
19. Liang, Z.; Li, Y.; Zhao, Z.; Xu, L.; Tang, Z. Monitoring mathematical model of grain cleaning losses on longitudinal-axial flow combine harvester. *Trans. Chin. Soc. Agric. Mach.* **2015**, *46*, 106–111.
20. Wang, J.; Li, F. Signal processing methods in fault diagnosis of machinery—Analyses in frequency domain. *Noise Vib. Control.* **2013**, *33*, 173–180.
21. Wang, J.; Li, F. Review of signal processing methods in fault diagnosis for machinery. *Noise Vib. Control.* **2013**, *33*, 128–132.
22. Hanping, M.; Wei, L.; Han, L.; Xiaodong, Z. Design of intelligent monitoring system for grain cleaning losses based on symmetry sensors. *Trans. Chin. Soc. Agric. Eng.* **2012**, *28*, 34–39.
23. Zhou, L.; Zhang, X.; Liu, Y.; Yuan, Y. Design of PVDF sensor array for grain loss measuring. *Trans. Chin. Soc. Agric. Mach.* **2010**, *41*, 167–171.
24. Zheng, Y.; Yang, Y.; Jia, D.; Xing, L.; Zhu, Y. Optimal Design of Voltage-controlled Voltage Source Second-order Unit Gain Butterworth High-pass Filter. *Electron. Technol.* **2012**, *39*, 33.
25. Williams, A.B. *Analog Filter and Circuit Design Manual*; Electronics Industry Press: Beijing, China, 2015; pp. 108–131.
26. Ma, X.; Cheng, X.; Hou, W. Simulation of diode peak value envelope detector based on Multisim 10.1. *Exp. Technol. Manag.* **2012**, *29*, 85–87.
27. Zhou, H.; Lv, Z.; Ma, G.; Hu, J. Experimental study of voltage comparator. *Exp. Technol. Manag.* **2012**, *29*, 42–44.

Disclaimer/Publisher’s Note: The statements, opinions and data contained in all publications are solely those of the individual author(s) and contributor(s) and not of MDPI and/or the editor(s). MDPI and/or the editor(s) disclaim responsibility for any injury to people or property resulting from any ideas, methods, instructions or products referred to in the content.